Laser Light Scattering Study of Microemulsion-like Polymerization Processes with Block Copolymers as Dispersants

Tianbo Liu,[†,‡] Horst Schuch,[*,†] Matthias Gerst,[†] and Benjamin Chu[*,‡,§]

Polymers Laboratory, BASF AG, D-67056, Ludwigshafen, Germany, Department of Chemistry, State University of New York at Stony Brook, Stony Brook, New York 11794-3400, and Department of Materials Science and Engineering, State University of New York at Stony Brook, Stony Brook, New York 11794-2275

Received March 17, 1999; Revised Manuscript Received June 18, 1999

ABSTRACT: Laser light scattering (LLS) was employed to monitor the microemulsion-like polymerization processes by using poly(methyl methacrylate)-*b*-poly(methacrylic acid) (P(MMA-*b*-MAA)) block copolymers with different block lengths (MMA_{58}-*b*-MAA_{57}, MMA_{67}-*b*-MAA_{217}, and MMA_{32}-*b*-MAA_{69}) or sodium dodecyl sulfate (SDS) surfactant as dispersants. A combination of static and dynamic light scattering techniques (SLS and DLS) was used to monitor the microemulsion-like systems before, during, and after polymerization. The polymerization of MMA (methyl methacrylate) was found to occur first in the dispersing aqueous medium, and then it was transferred inside the micellar cores to continue the polymerization process, which is similar to the homogeneous nucleation mechanism found when using small-molecule surfactants as dispersants. Depending on the hydrophobicity of the micellar cores, a rearrangement of micellar chains was found to take place during the different stages of the polymerization process. The similarities and differences of the dispersants between SDS surfactant micelles and P(MMA-*b*-MAA) block copolymer micelles are discussed. The polymerization of *n*-BA in micellar solution was also studied and compared with that of MMA.

Introduction

Microemulsion polymerization has been developed rapidly since the early 1980s as an important method for polymer synthesis. It has many unique advantages[1], such as large overall interfacial area (100 m^2/mL), optical transparency, small domain sizes (≈10 nm), and a great variety of structures.[2−4] Microemulsions are thermodynamically stable and isotropic dispersions containing oil, water, and surfactants, with the stability being ensured by a low interfacial tension, capable of compensating for the dispersion entropy. Short chain amphiphilic surfactants that usually contain a polar head and a long, organic chain for each molecule, e.g., SDS, are the commonly used dispersants. The dispersed phase provides a microenvironment for polymerization.[1] The surfactant chains can self-assemble into micellar structures that usually can stabilize solvent-phobic monomers. During the polymerization process, the micellar particles with polymers in the micellar cores grow by collisions between these particles and by monomer diffusion through the continuous dispersing phase. After polymerization, the final products are larger sized (about 40 nm) latex particles that consist of polymer chains surrounded by surfactant molecules. It has been reported that each latex particle contains only few (approaching one) polymer chains in water/oil microemulsion polymerization processes, the number was found to increase slightly with the degree of conversion in the case of oil/water microemulsions.[1,5−7] In microemulsion polymerization, the number of final latex particles has been found to be about 2 or 3 orders of magnitude less than the number of surfactant micelles before polymerization.[8]

Amphiphilic block copolymers have been considered as another type of dispersant.[9−15] The self-assembly behaviors of block copolymers in a selective solvent which is good for one block but a nonsolvent for another block have been widely reported.[16−18] The use of block copolymers instead of normal surfactants as dispersants can further extend the applications of microemulsion polymerization. New features can be introduced; e.g., domains can be cross-linked to produce membranes with compartmental structures.[9] Block copolymers have richer phase diagrams than normal surfactants and can be further modified. Therefore, they can provide more extended applications in this field in the future.

The microemulsion polymerization process has been investigated by Raman spectroscopy,[19] a pulsed UV laser source,[20] the rotating sector technique,[21] calorimetry, internal reflectance spectroscopy,[22] and other physical techniques. SLS was also employed to provide on-line information during the microemulsion polymerization process, as shown by Elbing et al.[23] The change in the scattered intensity as a function of polymerization time can be used to follow the polymerization process. Kourti et al.[24] used DLS to monitor the latex particle growth during microemulsion polymerization. Automatic sampling at every 10−15 min was performed. However, these early attempts did not extensively take advantage of the laser light scattering (LLS) techniques so that the information obtained was quite limited. Moreover, in most cases, SLS and DLS were used only to characterize the final product, the latex particles, yielding information on latex mass, size, and size distributions. The combination of SLS and DLS with other techniques, including solid-state NMR, transmission electron microscopy (TEM), small-angle X-ray scattering (SAXS) and small-angle neutron scattering

[†] BASF AG.
[‡] Department of Chemistry, State University of New York at Stony Brook.
[§] Department of Materials Sciences and Engineering, State University of New York at Stony Brook.

10.1021/ma990403n CCC: $18.00
Published on Web 09/03/1999

(SANS), has allowed the characterization of final products to become a routine and mature procedure.[25−29]

In this paper, we report the use of amphiphilic block copolymers P(MMA-*b*-MAA) (poly(methyl methacrylate)-*b*-poly(methacrylic acid)) as dispersants for microemulsion-like polymerization of poly(methyl methacrylate) (PMMA) and the preparation of poly(*n*-butyl acrylate) [P(*n*-BA)]. We used the term "microemulsion-like polymerization" because the polymerization investigated showed many features that were the same as those in a microemulsion polymerization process. However, before polymerization, there were no tiny monomer droplets in solution because of the low monomer concentration.[1] We shall use the term "microemulsion polymerization" from here on for convenience. The block copolymers have both hydrophobic and hydrophilic blocks that can act as dispersants similar to traditional surfactants. To our knowledge, this is the first time that a thorough comparison of the similarities and differences between block copolymers and surfactants in their roles as dispersants in microemulsion polymerization processes has been presented. Also, the whole process was monitored by a combination of SLS and DLS techniques. Although LLS has been used in the past to monitor microemulsion polymerization processes, information was obtained by using either SLS *or* DLS. Here we want to present the use of LLS as a probe. By a proper combination of SLS *and* DLS measurements, this technique can provide very rich information that is useful to monitor different stages of the microemulsion polymerization process. It should be noted that in reality, microemulsion polymerization reactions are often used at high monomer concentrations (suspensions or droplets). However, due to the special emphasis of the light-scattering technique to detect the presence of large particles, with the scattered intensity being proportional to the sixth power of particle size, LLS cannot be used easily to monitor the changes in an environment where large monomer droplets, in addition to the microemulsions, are present in the dispersing medium. Therefore, we used monomer concentrations that were sufficiently low in order to avoid the presence of monomer droplets, if any. We believe that the conclusions we draw here can also be applied to describe large-scale microemulsion polymerization processes at higher monomer concentrations, because there should be little difference in the chemical activity of monomers as a function of monomer concentration.

The microemulsion polymerization of MMA represents a typical oil-in-water microemulsion process for a water-soluble monomer. Its mechanism has been extensively discussed in earlier papers by using different physical techniques.[30−34] A two-step homogeneous nucleation mechanism was presented:[35] the monomers first started to polymerize in the continuous aqueous phase, and then the oligomers would be transferred into the dispersed phase where polymerization would continue. In this paper, we report in situ monitoring of the polymerization by means of LLS and a study on the similarities and differences of the MMA polymerization mechanism by using block copolymer micelles, instead of small-molecule surfactants, as dispersants.

Experimental Section

Sample Preparations. The samples MMA_{58}-*b*-MAA_{57}, MMA_{67}-*b*-MAA_{217} and MMA_{32}-*b*-MAA_{69} were prepared by living anionic polymerization at BASF AG and the University of Mainz, Mainz, Germany.[35] The SDS surfactant (>99%) was purchased from Fluka. A detailed description of the block copolymers and the SDS surfactant is listed in Table 1. Some work on characterizing P(MMA−MMA) micelles and exploring their applications has been reported before.[36] All polymer and surfactant solutions were controlled at pH = 11 by using NaOH.

Microemulsion polymerization of MMA and *n*-BA monomers took place at 80 °C. The sample solutions containing monomers and dispersant were first filtered, thus dust-free, into the 30 mm o.d. light-scattering cells by using 0.22 μm pore-size Millipore sterile filters. Then, in a water bath at 80 °C, the initiator (dust-free $Na_2S_2O_8$ in aqueous solution with the concentrations listed in Tables 3−6) was added into the sample solution. The light-scattering cell containing the monomers, the dispersant, and the initiator was then put into the sample chamber (maintained at 80 °C) of the LLS spectrometer for measurements.

Laser Light Scattering (LLS). We used a standard, laboratory-built light scattering spectrometer of ALV/Langen, Germany, (a Nd:YAG-Laser, 532 nm, 400 mW, Adlas) capable of both absolute integrated scattered intensity and photon

Table 1. General Descriptions of P(MMA-*b*-MAA) Block Copolymer Samples and SDS Surfactant

	block copolymer or surfactant	M_n	M_w/M_n	M_w
ZK 706/38	MMA_{58}-*b*-MAA_{57}	10 700	1.33	14 200
B51, ZK 1191/2949	MMA_{67}-*b*-MAA_{217}	25 400	1.06	27 000
B39	MMA_{32}-*b*-MAA_{69}	9100	1.32	12 000
SDS (sodium dodecyl sulfide)	$(H(CH_{12}))SO_3Na$			288

Table 2. Change of Micellar Aggregation Number (N_w) and Micellar Size ($2R_h$) in the Presence of MMA Monomers

	25 °C		80 °C	
	N_w	$2R_{h,90}$ (nm)	N_w	$2R_{h,90}$ (nm)
P(MMA-*b*-MAA) (1.0 g/L)	48	26.8	25	34.8
+MMA (1.0 g/L)	40	29.0	24	33.0
+MMA (10.0 g/L)	28	33.4	17	30.4

Table 3. Microemulsion Polymerization of MMA Monomer with MMA_{58}-*b*-MAA_{57} Block Copolymer as Dispersant (for Pure MMA_{58}-*b*-MAA_{57} Micelles, $N_w = 25$ and the Micellar Mass $M_{w,BC} = 3.5 \times 10^5$ g/mol)

MMA_{58}-*b*-MAA_{57}/ MMA concn (g/L) ($Na_2S_2O_8$ concn (g/L))	starting reacn time (min)	$2R_h$[a] (after reacn)	scattd intens (after reacn, I_{sol}/I_{tol})	final latex mass (Da)[c]	no. of copolym chains per latex[c]
1.0/1.0 (0.1)	20	32−33	5	3.5×10^5	12
1.0/2.4 (0.1)	15	32	22	7.2×10^5	15
1.0/5.0 (0.1)	13	38	115	2.2×10^6	26
1.0/5.0 (0.05)	25	41−42	137	2.9×10^6	41
5.0/5.0 (0.1)	14	30	44	4.1×10^5	14
1.0/10.0 (0.1)	12	47	505[b]	5.6×10^6	36

[a] From cumulants analysis. [b] After absorption correction. [c] 100% conversion rate.

Table 4. Microemulsion Polymerization of *n*-BA Monomer with MMA_{58}-*b*-MAA_{57} Block Copolymer as Dispersant

n-BA concn (g/L) ($Na_2S_2O_8$ concn (g/L))	starting reacn time (min)	$2R_h$ (after reacn)	scattered intens (after reacn, I_{sol}/I_{tol})	micellar mass (Da)[a]	no. of copolymer chains per latex[b]
1.0 (0.1)	28	31−32	5.2	9.0×10^5	13
3.0 (0.1)	34	35−36	24	1.8×10^6	16
1.0 (0.1) + 1.0 g/L MMA	20	31−32	11	5.6×10^5	13

[a] After reaction, 100% conversion rate. [b] 100% conversion rate.

Table 5. Microemulsion Polymerization of MMA Monomer with MMA_{67}-*b*-MAA_{217} Block Copolymer as Dispersant

P(MMA-*b*-MAA), MMA concn (g/L) ($Na_2S_2O_8$ concn (g/L))	starting reacn time (min)	$2R_h$[a] (after reacn)	scattd intens (after reacn, I_{sol}/I_{tol})	final latex mass (Da)[c]	no. of copolym chains per latex[c]
1.0−1.0 (0.1)	25		3.6	1.5×10^5	3
1.0−2.5 (0.1)	19	63	19	5.2×10^5	6
1.0−5.0 (0.1)	15	68	175	2.9×10^6	18
5.0−5.0 (0.1)	17		75	6.9×10^5	13
1.0−5.0 (0.05)	25	75	250	3.9×10^6	24
1.0−10.0 (0.1)	12	81	805[b]	7.5×10^6	25

[a] From CONTIN analysis. [b] After absorption correction. [c] 100% conversion rate.

Table 6. Microemulsion Polymerization of MMA Monomer with SDS Surfactant as Dispersant

SDS, MMA concn (g/L) ($Na_2S_2O_8$ concn (g/L))	starting reacn time (min)	$2R_h$[a] (after reacn)	scattd intens (after reacn, I_{sol}/I_{tol})	final latex mass (Da)[c]	no. of SDS per latex[c]
1.0−1.0 (0.1)	13		4		
1.0−2.5 (0.1)	12	28	60	1.7×10^6	1870
1.0−5.0 (0.1)	12	35	300	5.0×10^6	3130
5.0−5.0 (0.1)	9	19	47	5.1×10^5	960
1.0−5.0 (0.05)	18	37	315	5.2×10^6	3240
5.0−5.0 (0.05)	12	19	41	4.6×10^5	880
1.0−10.0 (0.1)	8	41	1100[b]	1.2×10^7	3600

[a] From cumulants and CONTIN analysis. [b] After absorption correction. [c] 100% conversion rate

correlation measurements at different scattering angles. SLS experiments were performed at scattering angles between 30 and 150°. DLS measurements were made by means of an ALV 5000 digital correlator. Measurements were usually performed at a scattering angle of 90°.

The basis for data analysis of SLS is the Rayleigh−Gans−Debye equation, valid for small, interacting particles in the form[37]

$$Hc/R_{90} = 1/M_w(1 + 2A_2c) \quad (1)$$

where $H \equiv 4\pi^2 n_{tol}^2 (dn/dc)^2/N_A\lambda^4$ is an optical parameter with n_{tol} being the refractive index of toluene, N_A being Avogadro's constant, λ being the laser wavelength (532 nm), M_w being weight-average molecular weight, A_2 being the second virial coefficient; and dn/dc being the refractive index increment. R_{90} is the excess Rayleigh ratio of the polymer solution at 90°, and it equals $R_{tol,90}(I - I_0)/I_{tol}(n^2/n_{tol}^2)$, where $R_{tol,90}$ is the Rayleigh ratio of toluene at 90°, with a value of 2.52×10^{-5}/cm at 532 nm[38] using vertically polarized incident and scattered light. I, I_0, and I_{tol} are the scattered intensities of the solution, the solvent, and toluene, respectively, and n is the refractive index of the solvent. From SLS measurements, we can determine M_w and A_2.

DLS[38] measures the intensity−intensity−time correlation function $G^{(2)}(\Gamma)$ by means of a multichannel digital correlator. The $G(\Gamma)$ so obtained can be used to determine an average apparent diffusion coefficient $<D_{app}>$, and the apparent hydrodynamic radius $R_{h,app}$ is related to D_{app} via the Stokes−Einstein equation:

$$D_{app} = kT/6\pi\eta R_{h,app} \quad (2)$$

k is the Boltzmann constant, and η is the solvent viscosity at temperature T. From DLS measurements, we can also obtain the particle size distribution in solution.

To monitor the microemulsion polymerization process, a combination of SLS and DLS was measured at a 90° scattering angle simultaneously, collecting experimental data of the total scattered intensity and particle size (cumulant method) every minute automatically during the experiment. The DLS results were then analyzed subsequently by the CONTIN method.[39]

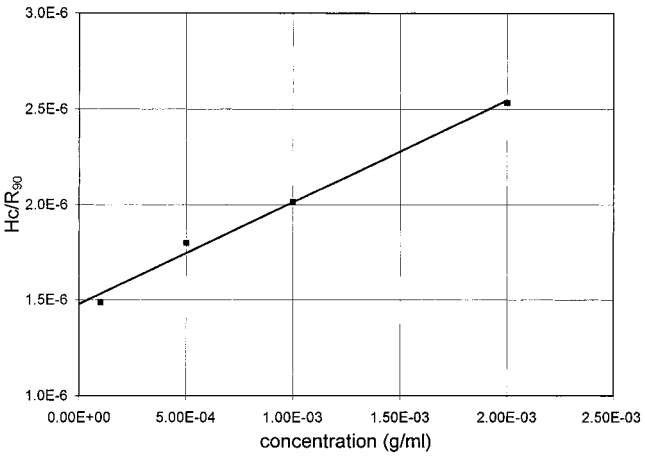

Figure 1. SLS measurements to determine the aggregation number (N_w) of MMA_{58}-*b*-MAA_{57} block copolymer micelles in aqueous solution at pH = 11 and 80 °C.

Results and Discussions

Part I. Characterization of P(MMA-*b*-MAA) Block Copolymer Micelles in Aqueous Solution without and with Additional Monomers. 1. Characterization of MMA_{58}-*b*-MAA_{57} Block Copolymer Micelles in Aqueous Solution. SLS and DLS measurements have become routine methods to obtain micellar properties in solution. For the total scattered intensity of polymer solutions at different concentrations, the cmc and the aggregation number (N_w) of micelles can be determined. For the MMA_{58}-*b*-MAA_{57} block copolymer, the cmc value is so small (≪0.1 g/L) that we can assume that all of the block copolymer chains in solution have formed micelles without introducing an appreciable error.

The dn/dc values of block copolymers were measured by using a laboratory-built refractometer, with dn/dc values being 0.150, 0.162, and 0.155 for MMA_{58}-*b*-MAA_{57}, MMA_{67}-*b*-MAA_{217}, and MMA_{32}-*b*-MAA_{69}, respectively. The dn/dc values of block copolymer micelles containing MMA or PMMA inside micellar cores can be obtained from the following equation:[40]

$$(dn/dc)_{P(MMA-b-MAA)} = \alpha(dn/dc)_{PMMA} + \beta(dn/dc)_{PMAA} + (1 - \alpha - \beta)(dn/dc)_{MMA} \quad (3)$$

In this equation, α and β are the weight fractions of PMMA and PMAA in the system, respectively. The dn/dc values of PMMA and PMAA polymers in water are 0.131 and 0.175 L/g, respectively.[41] The dn/dc of MMA is lower (0.093 L/g) than that of PMMA. For MMA monomers dissolved in water in the presence of P(MMA-*b*-MAA) micelles, most of them (about 90%) exist in the aqueous medium. This portion of MMA could not make an appreciable contribution to the total scattered intensity. Therefore, only a small portion of MMA inside the micellar cores needed to be considered. For the latex particles after polymerization, the dn/dc value was calculated by considering the masses of both the block copolymer chains and the newly formed PMMA chains inside each latex particle.

The N_w and the $2R_h$ values were obtained from SLS and DLS, respectively. Figure 1 shows the determina-

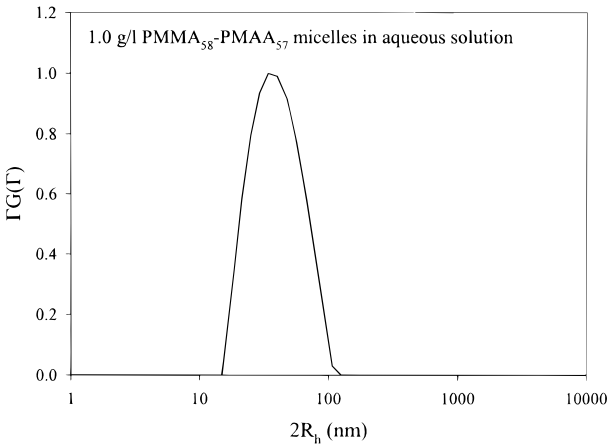

Figure 2. CONTIN analysis on DLS measurements of MMA_{58}-*b*-MAA_{57} block copolymer micelles in aqueous solution at pH = 11, 80 °C, and 90° scattering angle.

tion of M_w of the MMA_{58}-*b*-MAA_{57} block copolymer micelles at 25 °C. On the basis of eq 1, a value of 6.9×10^5 for M_w that was equivalent to 48 copolymer chains ($N_w = 48$) was determined. From 25 to 80 °C, there was an obvious decrease in the scattered intensity, suggesting a change in the micellar aggregation number (from 48 to 25). The glass transition temperature (T_g) of PMMA polymers were 105, 105, and 38 °C for atactic, syndiotactic and isotactic conformations, respectively.[42] At 25 °C, the PMMA blocks of the block copolymers (i.e., the micellar cores) were in the glassy state, while at 80 °C they could be above their T_g (>38 °C), suggesting that the micellar cores could become less rigid.

The change in $2R_h$ of copolymer micelles with increasing temperature can also be explained by checking the T_g of PMMA. A CONTIN analysis on DLS measurement of copolymer micelles was shown for example in Figure 2. The size distribution of the micelles was quite broad, suggesting a distribution of aggregation number in spite of the narrow polydispersity of chains; also aggregation of micelles might occur. The possible existence of a small amount of hydrophobic impurities may also result in a broad size distribution, as has been shown before.[43] From 25 to 80 °C, the $2R_h$ value of micelles increased from 27 to 35 nm, suggesting that the PMAA chains become more extended at higher temperatures.

The effect of additional electrolytes on the micelles was tested by preparing the micellar solutions in 0.1 N NaCl aqueous solution, to check the possible polyelectrolyte nature of PMAA blocks. However, the nature of the micelles (e.g., N_w and R_h values) did not indicate any substantial change when compared with that in a salt-free, pH = 11, environment. Therefore, in the following experiments, we always used the solutions without adding more salts.

The micellar size and the total scattered intensity remained essentially the same for pH values ranging from 10 to 12.

At 80 °C, the N_w of two other block copolymers, MMA_{67}-*b*-MAA_{217} and MMA_{32}-*b*-MAA_{69}, were 21 and 3, respectively. The length of the hydrophobic block played a dominant role in determining N_w, in agreement with our conclusions on block copolymer micelles in solution.[44−46]

2. MMA_{58}-*b*-MAA_{57} Micelles in the Presence of Different Monomers (MMA and *n*-BA). (1) Determination of Maximum Solubility of Monomers Inside Block Copolymer Micellar Cores. For some water-soluble monomers, e.g., MMA, their solubility in aqueous media cannot be neglected. The solubilization of different monomers in P(MMA-*b*-MAA) micelles were tested by visual observation. The solution became cloudy after continuously adding monomers into the copolymer solution. The maximum solubility of monomer in the micellar solution was subtracted by its solubility in water, the remaining amount should be considered as the amount of monomer dissolved inside the micellar cores. For 1 g/L MMA_{58}-*b*-MAA_{57} solution, the experiment showed that the majority of MMA was still in the aqueous media, due to its comparatively high solubility in water (15.6 and 16 g/L at 25 and 80 °C, respectively). 1 g/L MMA_{58}-*b*-MAA_{57} micelles can solubilize 1.0 g/L MMA or 1.2 g/L *n*-BA at 25 °C, and about 2−3 g/L and 1.5−2 g/L, respectively, at 80 °C (for *n*-BA, its solubility in water is 1.5 and 2.0 g/L at 25 and 80 °C, respectively).

(2) LLS Study of Micellar Solutions in the Presence of Monomers. We assume that the distribution coefficient of monomers inside block copolymer micellar cores and in the aqueous medium remains essentially constant at a fixed temperature when the monomer concentration is lower than its maximum solubility. By accepting this assumption, more quantitative results can be obtained from SLS measurements. At both 25 and 80°C, the N_w of micelles decreased with increasing monomer concentration. The results are shown in Table 2.

With the addition of monomers, a slight change in the $2R_h$ value was observed. At 25 °C, the $2R_h$ value increased with increasing amount of monomers; while at 80 °C, the trend was reversed. The results could involve two different processes. At 25 °C, the pure micelles were in the "frozen" state. Adding monomers into the solution lowered the T_g of PMMA block. Therefore, the micelles became softer and more swollen. However, at 80 °C, the P(MMA-*b*-MAA) micellar cores were already in the amorphous (soft) state. Therefore, the addition of monomers did not have a large effect to further increase the micellar size. On the contrary, a decrease in the aggregation number due to the addition of monomers should decrease the micellar size a little.

Part II. Using SLS and DLS To Monitor Microemulsion Polymerization with MMA_{58}-*b*-MAA_{57} Being the Dispersant. 1. Date Interpretation from LLS Measurements. A typical file for the polymerization of 5.0 g/L MMA with 1.0 g/L MMA_{58}-*b*-MAA_{57} and 0.1 g/L $Na_2S_2O_8$ initiator at pH 11 and 80 °C is shown in Figure 3. A sudden increase in the scattered intensity from on-line SLS measurements was detected about 12 min after the initiator was added into the solution, and over a short period of time (5−7 min) the total scattered intensity increased drastically, until finally it reached a stable value. We have to realize that this scattered intensity vs reaction time profile does not reveal the real conversion rate of monomers in solution, because of the special emphasis of light scattering; i.e., it is very sensitive to the presence of large particles. As discussed earlier, before polymerization, most of the monomers existed in the aqueous dispersing phase. Therefore, it should be expected that polymerization occurred first in the aqueous dispersing phase. However, due to the small molecular weight of MMA monomers (100), the oligomers in aqueous medium, if any, would be too small to be detected in terms of the total scattered intensity, even if the polymerization process had occurred. The change in the scattered intensity could be detected only

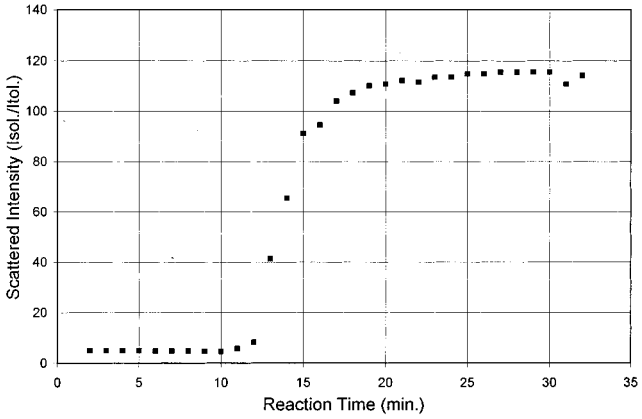

Figure 3. Time dependence of total scattered intensity of micellar solution during microemulsion polymerization (1 g/L MMA_{58}-*b*-MAA_{57} block copolymer, 5 g/L MMA monomer, 0.1 g/L $Na_2S_2O_8$ initiator at 80 °C, 90° scattering angle), with on-line SLS measurements.

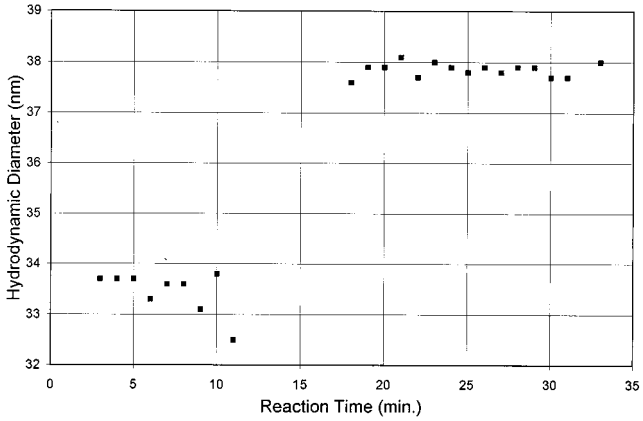

Figure 4. Time dependence of hydrodynamic diameter ($2R_h$) of copolymer micelles during microemulsion polymerization (1 g/L MMA_{58}-*b*-MAA_{57} block copolymer, 5 g/L MMA monomer, 0.1 g/L $Na_2S_2O_8$ initiator at 80 °C and 90° scattering angle), with on-line DLS measurements with cumulants analysis.

after the oligomers had grown to a certain size so that their solubility in water became unfavorable and they had to enter into the micellar cores for stabilization. As reported by Bléger et al.,[30] the "retardation" in the initial period on the microemulsion polymerization of MMA also existed with small-molecule surfactants. They monitored the reaction process by HPLC and on-line densimetry, and obtained experimental results quite similar to those obtained by us. They proposed that the polymerizaiton of MMA in aqueous surfactant solution followed the "homogeneous nucleation mechanism". In this mechanism, polymerizaiton of MMA first occurred in the aqueous medium. When the oligomers were long enough, they would be transferred to the dispersed phase in the microemulsion and continue to polymerize but at a much higher speed. This mechanism can also be applied here to show why the scattered intensity in the first 12 min of polymerization remained unchanged. It indicated the period when polymerization occurred mainly in the aqueous dispersing phase. The SLS results prove that polymerizations of MMA in the presence of surfactant micelles and block copolymer micelles are quite similar. The formation of oligomers from MMA unimers in aqueous medium should increase the total scattered intensity a little. However, this slight increase was covered by the strong scattered intensity of MMA_{58}-*b*-MAA_{57} block copolymer micelles (M_w over 5M).

To further prove the above conclusion, a parallel experiment was performed by using the same experimental conditions, but without adding any MMA_{58}-*b*-MAA_{57} block copolymer. On line SLS measurement showed that a slight but continuous increase in the scattered intensity could be observed during the first 5 min after the addition of initiators. This change could be attributed to be the early step of the polymerization process in the aqueous medium. Later, the sample became totally turbid.

There was a small amount of inhibitor existing with MMA and *n*-BA monomers (10−50 ppm). However, the amount of inhibitor was so tiny compared with the amount of initiator (e.g., for 5 g/L MMA and 0.1 g/L $Na_2S_2O_8$, the weight ratio was about 1:1000) that any delay time in polymerization could not be caused by inhibitor.

After the initial polymerization period, a drastic increase in the scattered intensity was observed in each experiment, suggesting that the formation of new homopolymer chains (much more hydrophobic than monomer) had been incorporated into the micellar cores. By assuming a 100% conversion rate and a very small cmc for the block copolymer, the molecular weight of the latex particles can be calculated by modifying eq 1

$$4\pi^2 n_{tol}^2 (dn/dc)^2 I_{tol}(C_{P(MMA-b-MAA)} + C_{PMAA})/[R_{tol}\lambda^4 N_A(I_{sol} - I_0)] = 1/M_{w,latex} \quad (4)$$

with $C_{P(MMA-b-MAA)}$ and C_{PMMA} being the concentrations of P(MMA-*b*-MAA) block copolymer and of the new PMMA polymer (or of MMA monomer before reaction) in solution, respectively, I_{sol} being the solution scattered intensity (after adsorption correction, if necessary) and I_0 being the solvent scattered intensity. In eq 4, an approximation was to drop the $2A_2C$ term. From eq 4 the weight-average mass of latex particles after polymerization ($M_{w,latex}$) can be calculated. By assuming that all of the block copolymer chains joined into latex particles, the number of copolymer chains per latex particle ($N_{BC,latex}$) can be calculated as

$$N_{BC,latex}M_{BC} = M_{w,latex}C_{P(MMA-b-MAA)}/(C_{P(MMA-b-MAA)} + C_{PMMA}) \quad (5)$$

where M_{BC} is the molecular weight of MMA_{58}-*b*-MAA_{57} copolymer micelles and $M_{w,latex}$ is the molecular weight of MMA_{58}-*b*-MAA_{57} block copolymer. The total mass of new PMMA polymer chains per latex particle can also be calculated by subtracting the mass of block copolymer chains in one latex particle from the total mass of the latex particle.

Figure 4 shows the cumulant analysis results of DLS measurements that were executed every minute during the polymerization process, under the same conditions as shown in Figure 3. The information on the $2R_h$ after polymerization (i.e., at times greater than 30 min) represents the average diameters of the final latex particles. In Figure 4, the $2R_h$ values corresponding to the 12th to the 17th min of polymerization were not available. The reason was that, during this period, the total scattered intensity was increasing and fluctuating drastically, suggesting a serious inhomogeneity in the solution during this period, and the PMMA chains started to enter into the micellar cores. The cumulant analysis could not give reasonable results with a

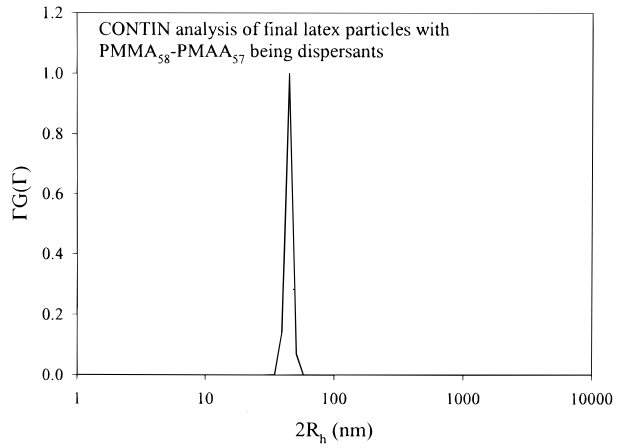

Figure 5. CONTIN analysis of DLS measurements on the final latex particles after polymerization of 1 g/L MMA_{58}-*b*-MAA_{57} block copolymer, 10 g/L MMA monomer, and 0.1 g/L $Na_2S_2O_8$ initiator, at 80 °C and 90° scattering angle.

continuously changing scattered intensity. This observation implied that the whole system had not reached equilibrium. Some extra large and insoluble particles (mainly due to newly polymerized hydrophobic PMMA chains) had formed in solution. The intensity fluctuations subsided after the polymerization, suggesting that the extra large particles had been solubilized by the block copolymer microemulsion.

The latex particles after polymerization had a very narrow size distribution. A typical CONTIN result is shown in Figure 5. When compared with the broad size distribution of the micelles before polymerization, the difference can be explained as that the presence of newly formed very hydrophobic PMMA chains had the effect of making the micelles more uniform in size by inducing a more hydrophobic micellar core and a sharper micellar core−shell interface. Under the current condition, the diameter of the final latex particles was about 38 nm, higher than that of the micelles before polymerization (33 nm). This difference revealed a growth of the micellar cores.

2. Effect of MMA Concentration. Figures 6 (SLS) and 7 (DLS) show the difference with different MMA concentrations. The time needed for observing the sudden increase in the total scattered intensity decreased with increasing MMA concentration, from the 12th min for 10.0 g/L MMA to about the 20th min for 1.0 g/L MMA. Also, the time duration of the polymerization process was shortened with increasing MMA concentration. This phenomenon can be interpreted as that the speed of polymerization in solution became lower at lower monomer concentration. Therefore, it took monomers a longer time to form long polymer chains and then enter into the micellar cores.

For MMA polymerization with fixed copolymer (1.0 g/L) and initiator (0.1 g/L) concentrations, a higher MMA concentration led to larger micellar sizes (in $2R_h$) and a higher micellar mass of the final latex particles (much higher scattered intensity) after polymerization. At higher MMA concentrations, more PMMA polymer chains had to be incorporated into the limited number of block copolymer micelles. Therefore, larger latex sizes could be expected. This observation does not totally fit the observations made by Loh et al.[33] on the microemulsion polymerization of MMA with small surfactants, where a maximum R_h value was found by increasing the MMA concentration. It should be noted that our study was limited to dilute MMA concentrations. With a larger amount of PMMA chains inside the micellar cores, the cores became more hydrophobic and larger in size. Then, more P(MMA-*b*-MAA) copolymer chains would be needed to join into one micelle to stabilize the system.

At high MMA concentrations (e.g., 10 g/L), the final latex particle solutions were no longer transparent. Therefore, light absorption should be considered in order to estimate the correct total scattered intensity. A dilution experiment was done by just diluting the highly concentrated latex solutions into a fixed, reasonable concentration (e.g., equivalent to 5 g/L MMA). Then the scattered intensity was again measured. The latex particles were very stable and should not change during this dilution process.

Table 3 summarizes the experiments discussed above. When less hydrophobic MMA monomers were added into MMA_{58}-*b*-MAA_{57} micellar solutions, the N_w of micelles decreased; during the polymerization process, because the PMMA polymer chains became longer and longer (more and more hydrophobic), the N_w of micelle was increasing, until it finally reached an equilibrium state.

In Figures 6 and 7, small decreases in both the scattered intensity and in $2R_h$ occurred before the sudden increase in the scattered intensity (or $2R_h$) due to polymerization. We would like to attribute this observation as due possibly to the small amount of hydrophobic impurities in the copolymer sample. The hydrophobic impurities made the average size of pure copolymer micelles a little bigger. More importantly, broader size distributions were detected using both the CONTIN and the cumulant analysis. Furthermore, a higher scattered intensity was observed. In Table 3, the final latex particle sizes (about 31−32 nm) for 2.4 and 1.0 g/L MMA were even a little bit smaller than those of the original micelles (e.g., 33 nm) by cumulant analysis.

Our above calculations were based on two assumptions: 100% conversion rate and all final products were inside the micellar cores. Both of them were acceptable for general microemulsion polymerization processes. However, in the current case the solubility of MMA monomer (also PMMA oligomers) in aqueous solution was very high. If the initial monomer concentration was very low (e.g., 1.0 g/L), the assumptions above might not be valid because a comparatively large fraction of MMA monomers and PMMA oligomers would remain in the aqueous medium. The establishment of equilibrium during polymerization also took more time. With a lower MMA weight fraction inside latex particles, the calculated values in the last two columns of Table 3 will be higher. For example, if 70 wt % polymerized MMA was inside latex particles, the values should be doubled. This topic will be discussed later.

3. Effects of MMA_{58}-*b*-MAA_{57} Block Copolymer Concentration. The effects of copolymer concentration (1.0 and 5.0 g/L MMA_{58}-*b*-MAA_{57}) on the microemulsion polymerization of MMA are shown in Figures 8 and 9. Several features can be drawn: first, the system for the 5.0 g/L copolymer had a higher scattered intensity than that of the system for 1.0 g/L copolymer before polymerization, due to the higher micellar concentrations. However, the trend reversed after the polymerization due partly to the difference in the latex particle masses.

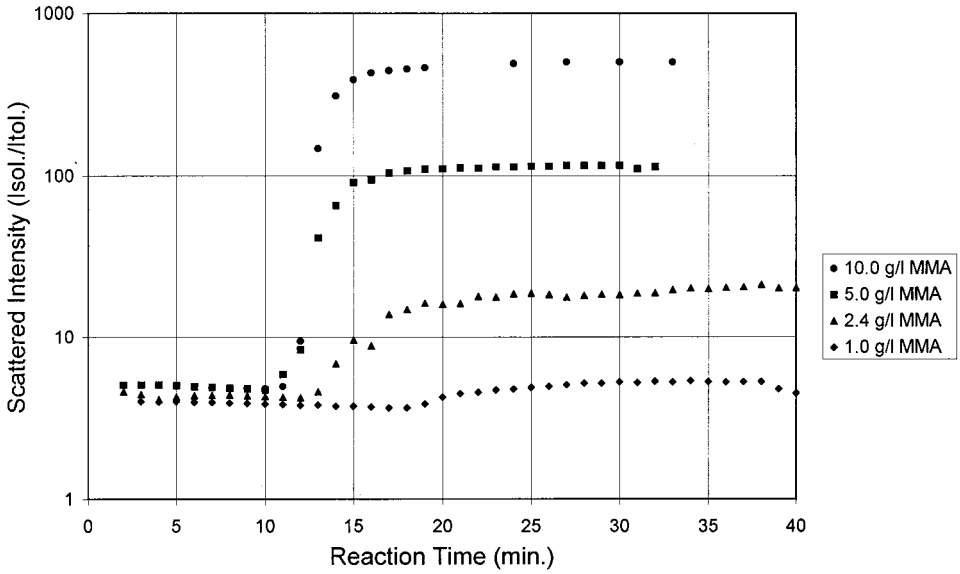

Figure 6. Time dependence of total scattered intensity of micellar solution during microemulsion polymerization: effect of MMA monomer concentration. On-line SLS measurements were performed in 1 g/L MMA_{58}-*b*-MAA_{57} block copolymer and 0.1 g/L $Na_2S_2O_8$ initiator, at 80 °C and 90° scattering angle.

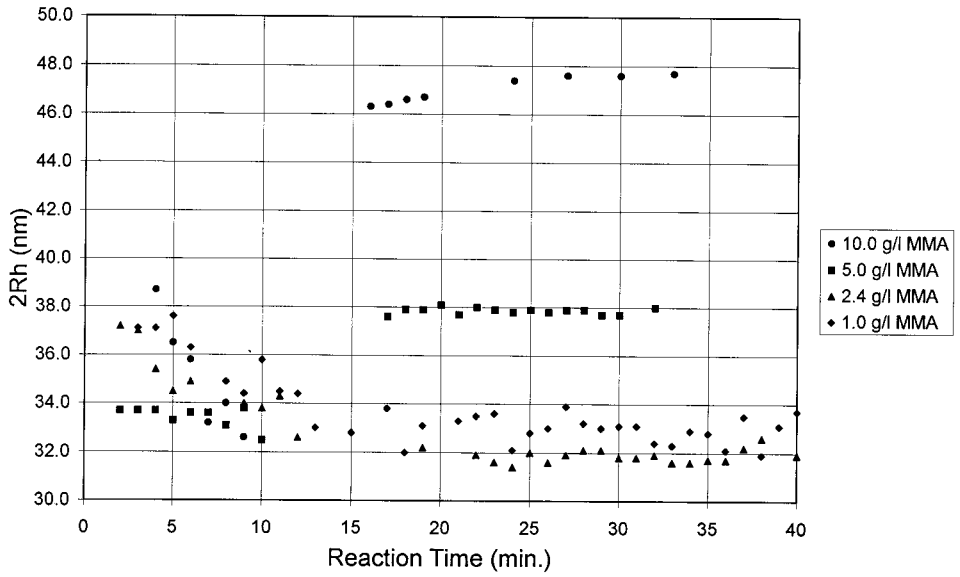

Figure 7. Time dependence of hydrodynamic diameter ($2R_h$) of copolymer micelles during microemulsion polymerization: effect of MMA monomer concentration. On-line DLS measurements were performed with cumulants analysis in 1 g/L MMA_{58}-*b*-MAA_{57} block copolymer and 0.1 g/L $Na_2S_2O_8$ initiator, at 80 °C and 90° scattering angle.

A smaller latex particle mass could be expected for the system with 5.0 g/L MMA_{58}-*b*-MAA_{57} because it provided more dispersants for the same amount of PMMA chains. A detailed calculation based on eqs 4 and 5 showed that the weight of newly formed PMMA chains in one latex for the 5.0 g/L copolymer system was equivalent to only $^1/_9$ of the weight in the system with 1.0 g/L copolymer. Also, one latex particle in the former system contained 14 copolymer chains while the latter one had 26 chains, because of the higher hydrophobicity. The difference in latex masses could also be proven by studying the latex sizes (Figure 9). The system with 1.0 g/L copolymer produced much larger latex particles (38 nm) than the system with 5.0 g/L copolymer (30 nm), as listed in Table 3. We did not observe the maximum $2R_h$ value in latex particle size by increasing the surfactant concentration, as reported by Loh et al.[33] at high surfactant concentrations (>8 wt %).

Figure 8 shows that the transition times of the scattered intensity for the two curves are quite similar, suggesting that the polymerization process was mainly controlled by the monomer concentration, but not by the copolymer concentration. This is another indirect evidence that the polymerization process first occurred mainly in the aqueous dispersion phase, instead of inside the micellar cores.

A comparison between the polymerization products of 5.0 g/L MMA_{58}-*b*-MAA_{57} + 5.0 g/L MMA monomers with that of 1.0 g/L MMA_{58}-*b*-MAA_{57} + 1.0 g/L MMA can reveal some information about the change in the conversion rate. Considering that these two systems have the same copolymer/monomer weight ratio, they should produce exactly the same latex particles if their conversion rate were the same. The only difference is in the number of latex particles (5:1), and therefore a 5:1 ratio in total scattered intensity can be expected after polymerization. However, experimentally we found

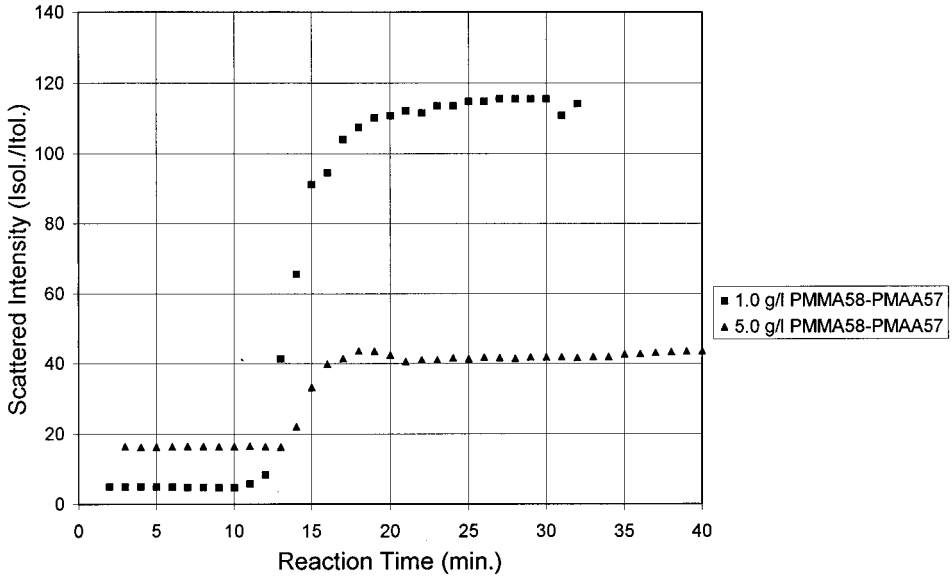

Figure 8. Time dependence of total scattered intensity of micellar solution during microemulsion polymerization: effect of MMA_{58}-*b*-MAA_{57} block copolymer concentration. On-line SLS measurements were performed in 5 g/L MMA monomer and 0.1 g/L $Na_2S_2O_8$ initiator, at 80 °C and 90° scattering angle.

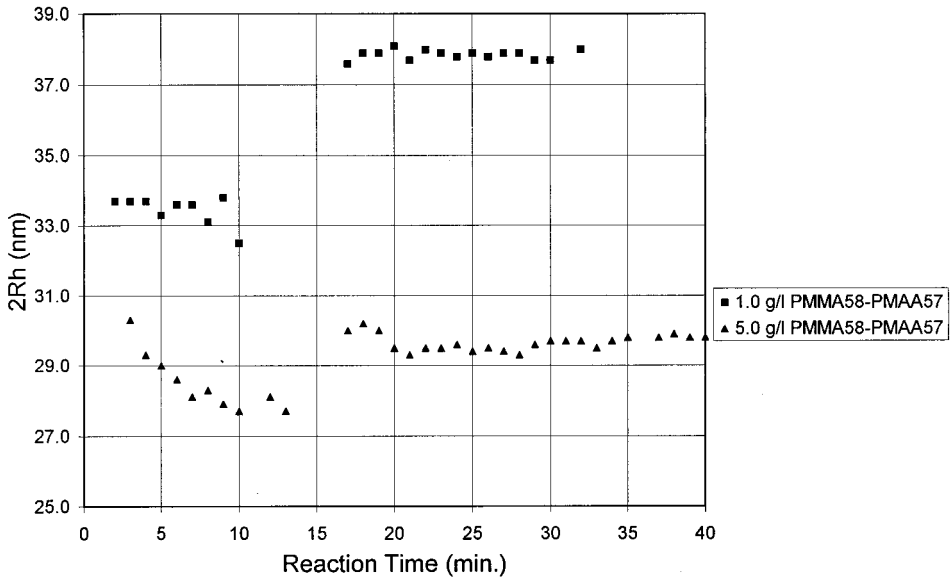

Figure 9. Time dependence of hydrodynamic diameter ($2R_h$) of copolymer micelles during microemulsion polymerization: effect of MMA_{58}-*b*-MAA_{57} block copolymer concentration. On-line DLS measurements were performed with cumulant analysis in 5 g/L MMA monomer and 0.1 g/L $Na_2S_2O_8$ initiator, at 80 °C and 90° scattering angle.

that the final total scattered intensity of the 5.0 g/L MMA system (Figure 8) was about 8−9 times higher than that of the 1.0 g/L MMA system (Figure 6). An explanation would be that, due to the PMMA oligomers staying in aqueous medium, a certain amount of PMMA could remain in the aqueous medium instead of entering the latex particles because of the comparatively high solubility of short-chain PMMA oligomers in water. However, the MMA solubility in water also had a limit. With 5.0 g/L MMA, the amount of PMMA oligomers remaining in water could not be 5 times higher than that in a 1 g/L MMA system because PMMA oligomers had reached its maximum solubility. Therefore, a higher weight fraction of newly formed PMMA polymer chains would be transferred into the latex particles and would lead to a higher total scattered intensity.

4. Effects of Initiator Concentration. The two curves in Figure 10 show the polymerization processes of 5.0 g/L MMA with 1.0 g/L MMA_{58}-*b*-MAA_{57}, but different $Na_2S_2O_8$ concentrations (0.1 and 0.05 g/L, respectively). Figure 11 shows a comparison of the same two systems in $2R_h$. When the $Na_2S_2O_8$ concentration decreased by half, the time needed for observing the sudden increase in scattered intensity was also about doubled, suggesting that the polymerization process became slower. At the same time, a lower initiator concentration also led to a little higher final mass of latex particles and larger latex sizes, suggesting a higher conversion rate for MMA monomers or a higher degree of polymerization. The latter conclusion is more plausible because there should be fewer radicals in solution at a lower initiator concentration. Then, fewer PMMA polymer chains were formed. Accordingly, the final PMMA polymer chains should be longer and also more hydrophobic. Therefore, each final latex particle would contain a higher mass of PMMA chains and need more copolymer chains to stabilize the system. The resultant effect was to enhance the total scattered

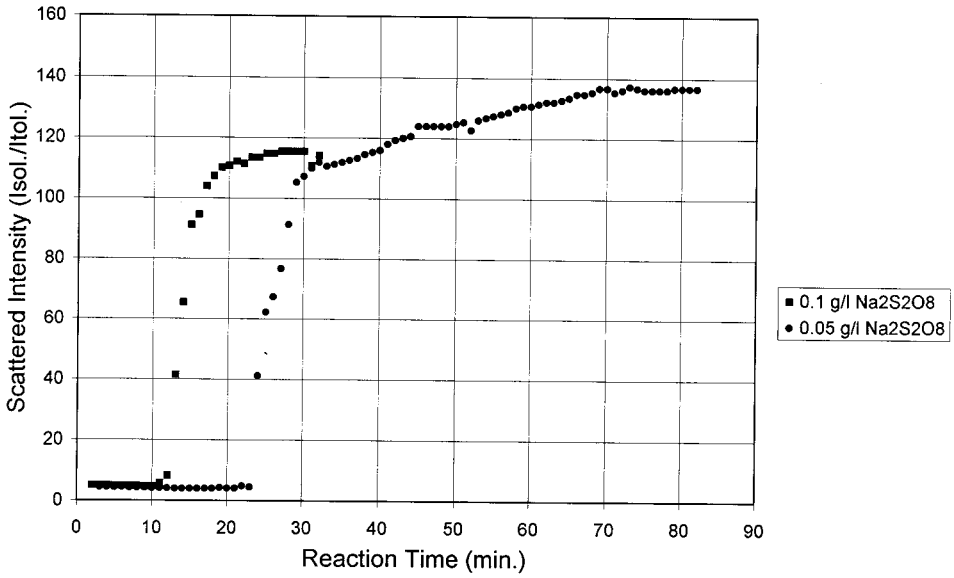

Figure 10. Time dependence of total scattered intensity of micellar solution during microemulsion polymerization: effect of $Na_2S_2O_8$ initiator concentration. On-line SLS measurements were performed in 1 g/L MMA_{58}-*b*-MAA_{57} block copolymer and 5 g/L MMA monomer, at 80 °C and 90° scattering angle.

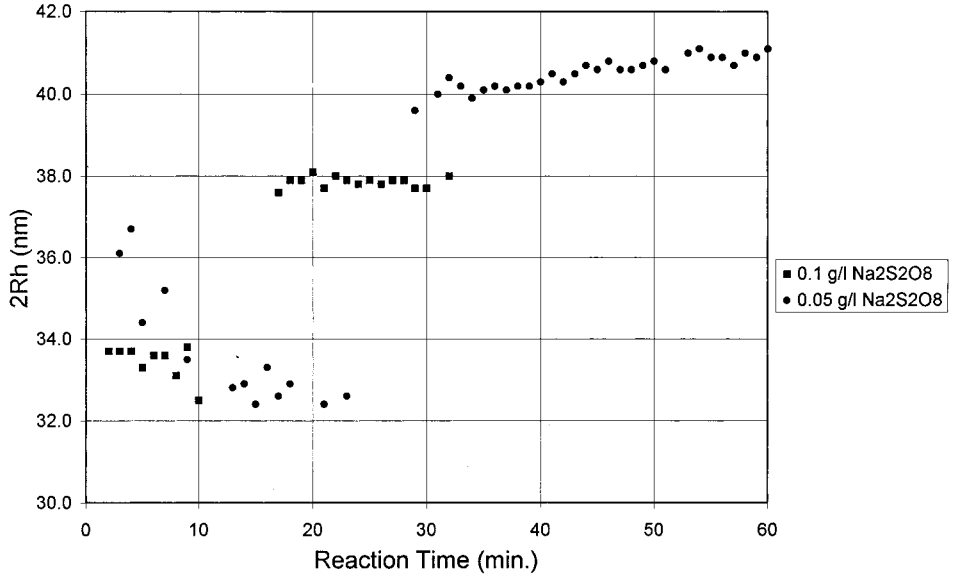

Figure 11. Time dependence of hydrodynamic diameter ($2R_h$) of copolymer micelles during microemulsion polymerization: effect of $Na_2S_2O_8$ initiator concentration. On-line DLS measurements were performed with cumulant analysis in 1 g/L MMA_{58}-*b*-MAA_{57} block copolymer and 5 g/L MMA monomer, at 80 °C and 90° scattering angle.

intensity. This conclusion is a little different from Gan et al.[32] as their initiator concentration did not affect the final latex particle size. The reason could be the fact that the LLS is a more sensitive tool to detect small changes. We did not observe a maximum rate of polymerization with increasing initiator concentration, as our study was carried out in the dilute solution regime.

On the basis of the discussions in the last several sections, the $2R_h$ and the N_w of final latex particles are interrelated. A higher N_w can be expected with a larger amount of MMA inside the latex particles, which could also lead to a larger latex particle size. The size of the latex particles was mainly determined by the concentration ratio of dispersant over monomer and the initiator concentration, which is consistent with conclusions made by other groups before.[7,31,34,47]

5. Reaction Speed of the Microemulsion Polymerization Process. By fixing the initiator concentration, the latent transition time in the total scattered intensity of 5.0 g/L MMA_{58}-*b*-MAA_{57} + 5.0 g/L MMA (14 min, Figure 8) was much shorter than that of 1.0 g/L MMA_{58}-*b*-MAA_{57} + 1.0 g/L MMA (20 min, Figure 6). However, it was about the same as those of 1.0 g/L P(MMA-*b*-MAA) + 5.0 g/L MMA (13 min, Figures 6 and 8) and 5.0 g/L MMA_{58}-*b*-MAA_{57} + 5.0 g/L MMA (14 min), suggesting that it was the MMA concentration that determined the speed of polymerization at a constant initiator concentration. The effect of MMA_{58}-*b*-MAA_{57} block copolymer concentration on the polymerization reaction rate was very minor.

The duration time of the polymerization process inside micelles (refer to the time span of the sudden increase in the scattered intensity) could also be determined by observing a plot of the scattered intensity vs reaction time. It is noted that when all of the parameters except the MMA concentration were fixed, the

Table 7. Comparison of Different P(MMA-*b*-MAA) Block Copolymers and SDS Surfactant as Dispersants in Microemulsion Polymerization (1.0 g/L dispersant, 10.0 g/L MMA, 0.1 g/L $Na_2S_2O_8$ at 80 °C)

	MMA_{67}-*b*-MAA_{217}	MMA_{58}-*b*-MAA_{57}	MMA_{32}-*b*-MAA_{69}	SDS
$N_{w,mic}$(pure micelle)	21	25	3	50
M_w[a]	7.5×10^6	5.6×10^6	8.2×10^6	1.2×10^7
$N_{w,latex}$[b]	25	36	62	3600
N_{latex} (per L)	8.9×10^{17}	1.2×10^{18}	8.1×10^{17}	5.8×10^{17}
$N_{w,mic}/N_{w,latex}$	1.2	1.4	21	72
$2R_h$(latex) (nm)	105	48	56	41
$2R_{h,core}$ (nm)	35	31	36	40
$2R_{h,shell}$ (nm)	70	17	20	1

[a] Weight of final latex. [b] Number of dispersant chains per latex.

duration time became lower (faster) at higher MMA concentrations, whereas the duration time remained basically constant at different concentrations of MMA_{58}-*b*-MAA_{57} copolymers. Therefore, the speed of the polymerization process was controlled by the MMA concentration (i.e., monomer diffusion) at constant initiator concentration.

6. Monitoring Polymerization Processes of *n*-BA. To compare the microemulsion polymerization behaviors of different monomers, another more hydrophobic monomer, *n*-butyl acrylate (*n*-BA), was also used to study the process by following the same experimental procedure mentioned above. For the polymerization processes of *n*-BA monomers in MMA_{58}-*b*-MAA_{57} solution, most of the rules mentioned above remained valid, as shown in Table 4.

The major difference between the polymerization processes with *n*-BA and MMA was that at higher *n*-BA concentrations (e.g., 3.0 g/L), the polymerization process could be detected at a later time (from Table 4) than that at lower *n*-BA concentrations (e.g., 1.0 g/L). Also, more block copolymer chains would be needed to stabilize the same amount of poly(*n*-BA) than that for PMMA due to the higher hydrophobicity of poly(*n*-BA) polymer chains (Tables 3 and 4). For the same reason, the 100% conversion rate might not be valid at low *n*-BA concentrations.

Part III. Polymerization of MMA with MMA_{67}-*b*-MAA_{217} or MMA_{32}-*b*-MAA_{69} Block Copolymers as Dispersants. SLS and DLS were used to study another pair of block copolymers with different block lengths, MMA_{67}-*b*-MAA_{217} and MMA_{32}-*b*-MAA_{69}, as dispersants for microemulsion polymerization. The cmc of MMA_{67}-*b*-MAA_{217} block copolymer micelles at 80 °C was very small, with an N_w of 21. The cmc of MMA_{32}-*b*-MAA_{69} was much higher (2 g/L) due to the short PMMA block length. The N_w of MMA_{32}-*b*-MAA_{69} at 80 °C was only 3, suggesting that the micelles were mainly molecular associates.

Qualitatively, the three block copolymers acted similarly as dispersants in the microemulsion polymerization process. Data similar to those in Table 3 for the MMA_{58}-*b*-MAA_{57} is summarized in Table 5 for MMA_{67}-*b*-MAA_{217}. A more detailed comparison will be given in a separate section and in Table 7.

Basically, the N_w during the microemulsion polymerization process was always changing, following the weight and composition changes of the micellar cores. The change of N_w suggested the change in the number of micelles in solution. This observation was consistent with the mechanism presented by Candau and coworkers that continuous particle nucleation occurred during microemulsion polymerization process.[48]

Part IV. Polymerization of MMA with SDS Surfactant. To make a comparison between block copolymers and common surfactants, studies on the microemulsion polymerization processes with SDS were also carried out. The SDS surfactant formed micelles in aqueous solution. At pH = 11 and 80 °C, the N_w of SDS micelles was about 50, obtained from SLS measurements. These micelles were only around 10 nm in size.

The monitoring of the microemulsion polymerization process with SDS by SLS and DLS gave similar results when compared with those using P(MMA-*b*-MAA) block copolymers as dispersants. The rearrangement of SDS chains per micelle during different stages of the polymerization process was also found. For the final latex particles, many SDS surfactant molecules (on the order of 1000) were needed to stabilize each latex particle. The concentration effects of monomer, surfactant and initiator followed the same rules as we had obtained in block copolymer systems, suggesting that these systems were quite similar; i.e., block copolymers acted as common surfactants in the microemulsion polymerization process. The results were summarized in Tables 6 and 7. For the final latex particles with SDS being dispersant, each particle contained around 2 orders of magnitudes more SDS chains than the N_w of pure SDS micelles; e.g., for 1 g/L SDS and 10 g/L MMA, the N_w of SDS micelles changed from 50 to 3600 after the polymerization process.

Part V. Comparison of Block Copolymers and SDS Surfactant, as Well as the Effects of Block Copolymer Lengths, in Microemulsion Polymerization Process. A major difference between P(MMA-*b*-MAA) micelles and SDS micelles in a microemulsion polymerization process came from the fact that block copolymer micelles seemed to be more "efficient" as a dispersant. As discussed above, the N_w value of a latex particle after polymerization depends on many factors: monomer concentration, copolymer concentration (or more accurately, the weight ratio of monomer to copolymer chains), initiator concentration, and length of different blocks, as well as other external conditions, e.g., temperature. The SLS study provides an estimate on the total average mass (M_w) of the final latex particles. The average N_w of the latex particle can also be obtained, as shown in Table 7. From Table 7, it is noted that the M_w of the latex particles and the number of latex particles in solution are quite similar for four different systems under the same polymerization conditions. However, when a comparison of the number of micelles before and after polymerization is made, the difference was quite clear. For the two block copolymers with longer hydrophobic blocks, the ratios of the numbers of micelles in solution before and after polymerization were close to 1, but for SDS, the number of latex particles in solution was 72 times fewer than that of micelles before polymerization. It suggested that block copolymer micelles, because of their highly hydrophobic

PMMA blocks and long hydrophilic chains, had a much stronger ability to stabilize the PMMA latex. On the other hand, the SDS surfactant, with a very short hydrophilic end, was less capable in this aspect. A general feature of microemulsion polymerization with traditional surfactants is that the number of latex is 2 or 3 orders of magnitude less than that of micelles before polymerization. If the two numbers were similar, this polymerization should be considered as "miniemulsion polymerization",[1] forming small latex particles (i.e., only a small amount of new PMMA was incorporated into each latex core). Then, even a small number of surfactants would be sufficient for stabilization. However, by using long chain P(MMA-*b*-MAA) block copolymers, we can synthesize latex particles with sizes equivalent to those obtained from the "microemulsion polymerization" process by using traditional surfactants, e.g., SDS. The amount of micelles with block copolymers was equivalent to the "miniemulsion polymerization" process with small-molecule surfactants.

Another difference between SDS and block copolymer micelles came from the "transition time" of polymerization from SLS measurements, i.e., the time that new PMMA oligomer chains started to be incorporated into micelles. With SDS, the "transition time" became earlier than that with P(MMA-*b*-MAA) micelles. One possibility is that the SDS micelles have much smaller hydrophilic parts, which can provide less of an obstacle effect during the transfer process of PMMA chains from the aqueous dispersing medium into the micellar cores.

In Table 7, the difference among the three block copolymers could also be explained. As MMA_{67}-*b*-MAA_{217} seemed to be a bit more efficient than MMA_{58}-*b*-MAA_{57} ($N_{mic}/N_{latex} = 1.2$ for the former one, and 1.4 for the latter one), fewer MMA_{67}-*b*-MAA_{217} chains were needed (25) to stabilize the same latex particles (for MMA_{58}-*b*-MAA_{57}, 36 copolymer chains were needed). Because they have similar PMMA block length, a longer PMAA length should have some effect of providing a higher capability for stabilization. At the same time, when comparing the efficiency of MMA_{32}-*b*-MAA_{69} ($N_{mic}/N_{latex} = 21$) with the other two, the difference is quite obvious. Therefore, we can conclude that the length of the hydrophobic block plays an important role in determining the N_w of micelles. This observation is coincident with the general understanding that the solvent-phobic block determines the micellar formation.

Table 7 also summarizes the results from DLS measurements. The $2R_h$ values of the final latex particles were obtained from the CONTIN analysis. For SDS latex particles, it was reasonable to assume that the diameter of the hydrophobic latex core was mainly responsible for the particle size since the SDS polar heads were quite short (in angstrom scale). We estimated that the size of the latex core was about 40 nm. From the data in Table 7, we could calculate the core size of the other latex particles under the same experimental conditions by using the relation

$$2R_{h,core,BC} = 2R_{h,core,SDS}\,(n_{BC,latex}/n_{SDS,latex})^{1/3} \quad (6)$$

with $2R_{h,core,BC}$, $2R_{h,core,SDS}$ (40 nm), $n_{BC,latex}$, and $n_{SDS,latex}$ being the core size and the number density of copolymer and SDS latex particles in solution, respectively. The data on the last line in Table 7 came from the difference in the data from the above two lines, giving the size of the latex shells. The shell thickness increased proportionally with certain exponential power with the length of the hydrophilic block length. This conclusion agrees well with the fact that hydrophilic blocks formed micellar shells and determined the size of the micellar shells.[44]

Conclusions

The combination of static and dynamic light scattering is an effective and powerful method to monitor the microemulsion polymerization process in dilute solution.

As dispersants, P(MMA-*b*-MAA) block copolymer micelles act similarly to that of SDS surfactant micelles. All of the micelles have the ability to solubilize a small amount of MMA monomers before polymerization. MMA form a distribution both inside micellar cores and in the aqueous dispersing medium. The presence of less hydrophobic MMA monomers decreases the N_w of micelles. Microemulsion polymerization of MMA first occurred in the aqueous dispersing medium. As the PMMA chains were too long and too hydrophobic to exist in the aqueous dispersing medium, they would transfer themselves into the micellar cores and the polymerization process was continued inside the micellar cores. With increasing PMMA chain length, more and more dispersant joined one latex particle to stabilize the system. The final products were homogeneous, stable and narrow size-distributed latex particles. More dispersants were needed in one latex particle to stabilize the same amount of more hydrophobic poly(*n*-BA) chains. The mechanism of microemulsion polymerization of MMA with block copolymers as dispersants is quite similar to the "homogeneous nucleation" mechanism, which was obtained with small-molecule surfactants being dispersants.

The length and hydrophobicity of the hydrophobic block played a key role in determining the number of copolymer chains per micelle before and after polymerization. Under the same external conditions, the change in N_w before and after polymerization was less serious (the micelles were more "efficient") with longer or more hydrophobic chains. The "efficiency" of P(MMA-*b*-MAA) block copolymers was much higher than that of the SDS surfactant.

The efficiency of micelles in microemulsion polymerization processes can be affected by the concentrations of block copolymer, monomer and initiator, the length and the type of blocks and the type of monomers, as well as external conditions, e.g., temperature. Higher efficiency can be achieved by increasing the hydrophobicity of the hydrophobic (PMMA) block, the lengths of both blocks, by decreasing the block copolymer/monomer ratio, the initiator concentration and by using less hydrophobic monomers.

Acknowledgment. We thank S. Jüngling (BASF AG) and W. Stauf and A. H. E. Müller (Department of Chemistry, University of Mainz) for synthesizing the block copolymers (S.J., MMA_{58}-*b*-MAA_{57}; W.S. and A.M., MMA_{67}-*b*-MAA_{217} and MMA_{32}-*b*-MAA_{69}). Their work was done within Research Project No. 03N3004 (finished 1997) of the German Ministry for Research, whose support is acknowledged. Thanks go to D. Urban (BASF AG) for encouraging this project and to K. Werle (BASF AG) for support in assembly and maintenance of the high-temperature LLS equipment and some initial experiments, which pointed to the feasibility of the

experiments. B.C. wishes to gratefully acknowledge partial support of this work by the National Science Foundation, Polymers Program (DMR 9612386), the U.S. Army Research Office (DAAG559710022), and the Department of Energy (DEFG0286ER45237.015).

References and Notes

(1) Candau, F. Microemulsion Polymerization. In *Polymeric Dispersions: Principles and Applications*; Asua, J. M., Ed.; Kluwer Academic Publishers: Dordrecht, The Netherlands, 1997 and references therein.
(2) Candau, F. Microemulsion Polymerization. In *Encyclopedia of Polymer Science and Engineering*, 2nd ed.; Mark, H. F., Bikales, N. M., Overberger, C. G., Menges, G., Eds.; 1987; Vol. 9.
(3) Candau, F. Polymerization in Microemulsions. In *Polymerization in Organized Media*; Paleos, C. M., Ed.; Gordon and Breach Publishers: Philadelphia, PA, 1992; Chapter 4.
(4) Antonietti, M.; Basten, R.; Lohmann, S. *Macromol. Chem. Phys.* **1995**, *196*, 441.
(5) Candau, F.; Leong, Y. S.; Pouyet, G.; Candau, S. J. *J. Colloid Interface Sci.* **1984**, *101*, 167.
(6) Guo, J. S.; El-Aasser, M. S.; Vanderhoff, J. M. *J. Polym. Sci., Polym. Chem. Ed.* **1989**, *27*, 691.
(7) Guo, J. S.; Sudol, E. D.; Vanderhoff, J. W.; El-Aasswe, M. S. *J. Polym. Sci., Polym. Chem. Ed.* **1992**, *30*, 703.
(8) Candau, F.; Leong, Y. S.; Fitch, R. M. *J. Polym. Sci., Polym. Chem. Ed.* **1985**, *23*, 193.
(9) Meier, W.; Falk, A.; Odenwald, M.; Stieber, F. *Coloid Polym. Sci.* **1996**, *274*, 218.
(10) Helmstedt, M.; Schaefer, H. *Polymer* **1994**, *35*, 3377.
(11) Stejskal, J.; Kratochvil, P. *Makromol. Chem., Macromol. Symp.* **1992**, *58*, 221.
(12) Mura, J.-L.; Riess, G. *Polym. Adv. Technol.* **1995**, *6*, 497.
(13) Piirma, I.; Sar, B. *Polym. Int.* **1993**, *30*, 145.
(14) Stejskal, J.; Kratochvil, P.; Koubik, P,; Tuzar, Z.; Helmstedt, M.; Jenkins, A. D. *Polymer* **1990**, *31*, 1816.
(15) Dawkins, J. V.; Taylor, G.; Baker, S. P.; Collett, R. W.; Higgins, J. S. *Org. Coat. Plast. Chem.* **1980**, *43*, 215.
(16) Chu, B.; Zhou, Z. In *Nonionic Surfactants: Polyoxyalkylene Block Copolymers*; Nace, V. M., Ed.; Marcel Dekker: New York, 1996; Chapter 3.
(17) Tuzar, K.; Kratochvil, P. In *Surface and Colloid Science*, Matijevic, E., Ed.; Plenum Press: New York, 1993; Vol. 15.
(18) Chu, B. *Langmuir* **1995**, *11*, 414.
(19) Feng, L.; Ng, K. Y. S. *Macromolecules* **1990**, *23*, 1048.
(20) Manders, B. G.; van Herk, A. M.; German, A. L.; Sarnecki, J.; Schomäcker, R.; Schweer, J. *Macromol. Chem. Rapid Commun.* **1993**, *14*, 693.
(21) Carver, M. T.; Dreyer, U.; Knoesel, R.; Candau, F.; Fitch, R. M. *J. Polym. Sci. Polym. Chem. Ed.* **1985**, *27*, 2161.
(22) Full, A. P.; Puig, J. E.; Gron, L. U.; Kaler, E. W.; Minter, J. R.; Mourey, T. H.; Texter, J. *Macromolecules* **1992**, *25*, 5157.
(23) Elbing, E.; Parts, A. G.; Lyons, C. J.; Coller, B. A. W.; Wilson, I. R. *Aust. J. Chem.* **1989**, *42*, 2085.
(24) Kourti, T.; MacGregor, J. F.; Hamielec, A. E.; Nicoli, D. F.; Elings, V. B. *Adv. Chem. Ser.* **1990**, *227*, 105.
(25) Fisher, L. W.; Melpolder, S. M.; O'Reilly, J. M.; Ramakrishnan, V.; Wignall, G. D. *J. Colloid Interface Sci.* **1988**, *123*, 24.
(26) Lacroix-Desmazes, P.; Guyot, A. *Colloid Polym. Sci.* **1996**, *274*, 1129.
(27) Kawaguchi, S.; Winnik, M. A.; Ito, K. *Macromolecules* **1996**, *29*, 4465.
(28) Full, A. P.; Kaler, E. W.; Arellano, J.; Puig, J. E. *Macromolecules* **1996**, *29*, 9, 2764.
(29) Hammouda, A.; Pileni, M. P. *Prog. Colloid Polym. Sci.* **1994**, *97*, 229.
(30) Bléger, F.; Murthy, A. K.; Pla, F.; Kaler, E. W. *Macromolecules* **1994**, *27*, 2559.
(31) Gan, L. M.; Chew, C. H.; Ng, S. C.; Loh, S. E. *Langmuir* **1993**, *9*, 2799.
(32) Gan, L. M.; Chew, C. H.; Lim, J. H.; Lee, K. C.; Gan, L. H. *Colloid Polym. Sci.* **1994**, *272*, 1082.
(33) Loh, S.-E.; Gan, L. M.; Chew, C.-H.; Ng, S.-C. *J. Macromol. Sci. Pure Appl. Chem.* **1995**, *A32*, 1681.
(34) Gan, L. M.; Lee, K. C.; Chew, C. H.; Ng, S. C. *Langmuir* **1995**, *11*, 449.
(35) Feldthusen, J.; Ivan, B.; Müller, A. H. E. *Macromolecules* **1997**, *31*, 5578.
(36) Urban, D.; Gerst, M.; Rossmanith, P.; Schuch, H. Presented at the 216th National Meeting of the American Chemical Society, Boston, MA, Aug 1998, and forthcoming papers.
(37) Hiemenz, P. Z. *Principle of Colloid and Surface Chemistry*; Marcel Dekker Inc.: New York, 1985.
(38) Chu, B. *Laser Light Scattering*, 2nd ed.; Academic Press: San Diego, CA, 1991.
(39) Provencher, S. W. *Biophys. J.* **1976**, *16*, 29; *J. Chem. Phys.* **1976**, *64*, 2772.
(40) Wu, G.; Zhou, Z.; Chu, B. *Macromolecules* **1993**, *26*, 2117.
(41) *Polymer Handbook*, 3rd ed., Part VII; John Wiley & Sons: New York, 1989.
(42) Zhou, Z.; Chu, B.; Nace, V. M. *Langmuir* **1996**, *12*, 5016.
(43) Liu, T.; Zhou, Z.; Wu, C.; Chu, B.; Schneider, D.; Nace, V. M. *J. Phys. Chem. B* **1997**, *101*, 8808.
(44) Liu, T.; Zhou, Z.; Wu, C.; Nace, V. M.; Chu, B. *J. Phys. Chem. B* **1998**, *102*, 2875.
(45) Liu, T.; Zhou, Z.; Wu, C.; Nace, V. M.; Chu, B. *Macromolecules* **1997**, *30*, 7624.
(46) *Polymer Handbook*, 2nd ed.; John Wiley & Sons Inc.: New York, 1975; p III 148.
(47) Perez-Luna, V. H.; Puig, J.-E.; Castano, V. M.; Rodriguez, B. E.; Murthy, A. K.; Kaler, E. W. *Langmuir* **1990**, *6*, 1040.
(48) Carver, M. T.; Hirsch, E.; Wittmann, J. C.; Fitch, R. M.; Candau, F. *J. Phys. Chem.* **1989**, *93*, 4867.

MA990403N